SEDIMENTOLOGY the journal of the International Association of Sedimentologists

Sedimentology (2017) **64**, 1488–1510 doi: 10.1111/sed.12361

Upstream control of river anastomosis by sediment overloading, upper Columbia River, British Columbia, Canada

BART MAKASKE*, EVA LAVOOI†, TJALLING DE HAAS†, MAARTEN G. KLEINHANS† and DERALD G. SMITH‡[1]

**Soil Geography and Landscape group, Wageningen University, P.O. Box 47, 6700 AA Wageningen, The Netherlands (E-mail: bart.makaske@wur.nl)*

†Department of Physical Geography, Faculty of Geosciences, Utrecht University, P.O. Box 80115, 3508 TC Utrecht, The Netherlands

‡Department of Geography, University of Calgary, Calgary, Alberta T2N 1N4, Canada

Associate Editor – Vern Manville

ABSTRACT

Anastomosing rivers, systems of multiple interconnected channels that enclose floodbasins, constitute a major category of rivers for which various sedimentary facies models have been developed. While the sedimentary products of anastomosing rivers are relatively well-known, their genesis is still debated. A rapidly growing number of ancient alluvial successions being interpreted as of anastomosing river origin, including important hydrocarbon reservoirs, urge the development of robust models for the genesis of anastomosis, to facilitate better interpretation of ancient depositional settings and controls. The upper Columbia River, British Columbia, Canada, is the most-studied anastomosing river and has played a key role in the development of an anastomosing river facies model. Two hypotheses for the origin of upper Columbia River anastomosis include the following: (i) downstream control by aggrading cross-valley alluvial fans; and (ii) upstream control by excessive bedload input from tributaries. Both upstream and downstream control may force aggradation and avulsions in the upper Columbia River. In order to test both hypotheses, long-term (millennia-scale) floodplain sedimentation rates and avulsion frequencies are calculated using ^{14}C-dated deeply buried organic floodplain material from cross-valley borehole transects. The results indicate a downstream decrease in floodplain sedimentation rate and avulsion frequency along the anastomosed reach, which is consistent with dominant upstream control by sediment overloading. The data here link recent avulsion activity to increased sediment supply during the Little Ice Age (*ca* 1100 to 1950 AD). This link is supported by data showing that sediment supply to the upper Columbia study reach fluctuated in response to Holocene glacial advances and retreats in the hinterland. Upstream control of anastomosis has considerable implications for the reconstruction of the setting of interpreted ancient anastomosing systems. The present research underscores that anastomosing systems typically occur in relatively proximal settings with abundant sediment supplied to low-gradient floodplains, a situation commonly found in intermontane and foreland basins.

Keywords Anastomosing river, avulsion, floodplain sedimentation, fluctuating sediment supply, foreland basin, intermontane basin, radiocarbon age determination.

[1]Derald G. Smith passed away on 18 June 2014.

INTRODUCTION

An anastomosing river can be defined as a river having multiple interconnected channels that enclose floodbasins (Makaske, 2001). Anastomosing rivers are commonly formed by avulsions, flow diversions that cause the formation of new channels on the floodplain. When the new channels rejoin the parent channel downstream, islands are formed, which consist of isolated portions of the floodplain. Over time, these islands develop central depressions because of natural levée accretion along the bounding channels (Adams *et al.*, 2004). With their concave-up morphology, the islands of anastomosing rivers function as floodbasins (Makaske, 2001, fig. 2), trapping fine sediments and commonly hosting wetlands (Smith, 1983). The typical morphology of their islands is a fundamental characteristic of anastomosing rivers, which makes them different from other rivers with multiple channels/thalwegs that exhibit convex-up islands or bars (Makaske, 2001). While the latter rivers may be classified as anabranching rivers, i.e. multichannel rivers with more or less stable islands or bars that reach up to bankfull or floodplain level (Nanson & Knighton, 1996), they are not anastomosing. Thus, anastomosing rivers constitute a subcategory of the larger category of anabranching rivers and can be distinguished on the basis of their specific island morphology. In addition to a unique geomorphology, anastomosing rivers share a typical assemblage of sedimentary products, which has been summarized in widely applied facies models (Smith, 1983; Makaske, 1998, 2001).

While the geomorphology and sedimentary products of anastomosing rivers are relatively well-known, the causes of their formation are not yet fully understood. In general, the formation of anastomosing rivers is attributed to two factors: (i) high bank stability, often influenced by riparian (tree) vegetation (e.g. Smith, 1973; Harwood & Brown, 1993; Davies & Gibling, 2011); and (ii) net aggradation, driving the creation of new channels by avulsion (Makaske *et al.*, 2009). The current debate on the origin of anastomosing rivers focuses on the controls of aggradation, being upstream or downstream (e.g. Abbado *et al.*, 2005; Kleinhans *et al.*, 2012). The identification of dominant upstream or, alternatively, dominant downstream control of aggradation is fundamental to modelling the depositional setting in which anastomosing rivers occur. Associated with dominant upstream control (by excessive sediment supply) is the occurrence of well-developed anastomosis in relatively proximal positions near sediment source areas. In contrast, dominant downstream control (by base-level rise) implies that well-developed anastomosis will occur in relatively distal positions near a (local) base level. Therefore, more insight into the nature of the controls on aggradation in modern anastomosing systems is needed to facilitate better interpretation of ancient depositional settings and controls.

Over the past three decades, the upper Columbia River, British Columbia, Canada, has played a prominent role in a series of studies of anastomosing river geomorphology and sedimentology (Smith, 1983; Makaske, 1998, 2001; Makaske *et al.*, 2002, 2009; Tabata & Hickin, 2003; Abbado *et al.*, 2005; Kleinhans *et al.*, 2012). Concepts derived from the upper Columbia River have been applied to modern, subrecent and ancient interpreted anastomosing systems, worldwide (many references in Makaske, 2001). The pioneering work in the upper Columbia River by Smith (1983) resulted in a well-established anastomosing river facies model that was later refined by Makaske (1998, 2001).

Upper Columbia anastomosis was initially believed to be caused by a rise in base level due to aggrading cross-valley alluvial fans (Smith, 1983). These cross-valley alluvial fans blocking the axial upper Columbia River were supposed to create backwater effects inducing low gradients and frequent overbank flooding, leading to high sedimentation rates in the valley upstream of the fans. The associated channel-belt aggradation was taken as a driving force of frequent avulsions creating the anastomosing river. Upper Columbia River anastomosis was thus considered as a product of downstream control. Abbado *et al.* (2005) challenged this notion of downstream control of upper Columbia River anastomosis and, mainly based on a morphological and river gradient analysis, proposed upstream control by sediment overloading from important tributaries. This hypothesis was confirmed in a sediment budget analysis by Makaske *et al.* (2009) and in a modelling study by Kleinhans *et al.* (2012). These studies, however, are based on an analysis of present-day morphology and hydraulic and sedimentary processes, and therefore are of little use for evaluating the long-term controls of anastomosis. Makaske *et al.* (2002)

demonstrated that upper Columbia anastomosis has existed for at least 3000 years and, consequently, an evaluation of its controls should ideally cover the same period of time. Another issue that demands a long-term perspective is that upstream control would require unsteady sediment supply from the hinterland, for which causes have not been investigated (Kleinhans *et al.*, 2012).

In this study, long-term floodplain sedimentation rates of the upper Columbia River have been determined in order to investigate the relative importance of upstream and downstream control on the millennia timescale. It is expected that in the case of dominant upstream control long-term floodplain sedimentation rate decreases downstream from important tributaries. The opposite is expected for the case of dominant downstream control through backwater effects induced by alluvial fans. A third option is that upstream and downstream control both equally influence upper Columbia River dynamics, in which case there would be no increase or decrease in long-term floodplain sedimentation rate along the system. An additional issue addressed in this paper is the timing of tributary sediment input in relation to catchment processes.

STUDY REACH AND PREVIOUS WORK

The upper Columbia River (bankfull discharge *ca* 220 m^3 sec^{-1} in the study reach) flows northwest through the Columbia Valley, which is part of the Rocky Mountain Trench in south-eastern British Columbia (Figs 1 and 2). The anastomosing reach is *ca* 100 km long and has developed in a tens of metres-thick unconsolidated valley fill. The upper Columbia floodplain in this reach is *ca* 1·5 km wide and flanked by mountain slopes and tributary valleys from which alluvial fans protrude into the Columbia Valley. One of the main cross-valley fans was formed by the Spillimacheen River, an important tributary draining the Purcell Mountains west of the Columbia Valley. Downstream of this fan, upper Columbia anastomosis is particularly well-developed with three to five parallel channels (Fig. 3A). This *ca* 20 km long reach (main channel distance) is characterized by high crevasse activity and a relatively steep average river channel slope of *ca* 16 cm km^{-1} (Abbado *et al.*, 2005). The lower *ca* 10 km of this reach is steepest with a channel slope of 21·5 cm km^{-1} (Fig. 4). Downstream of this reach, anastomosis is weakly developed with typically two to three parallel channels (Fig. 3B). This reach is *ca*

Fig. 1. The Rocky Mountain Trench with the anastomosing upper Columbia River, British Columbia, Canada. View looking ESE and up-valley from the Purcell Mountains with the Brisco Range of the Rocky Mountains in the background. Valley floor width in the middle of the photograph is *ca* 2 km.

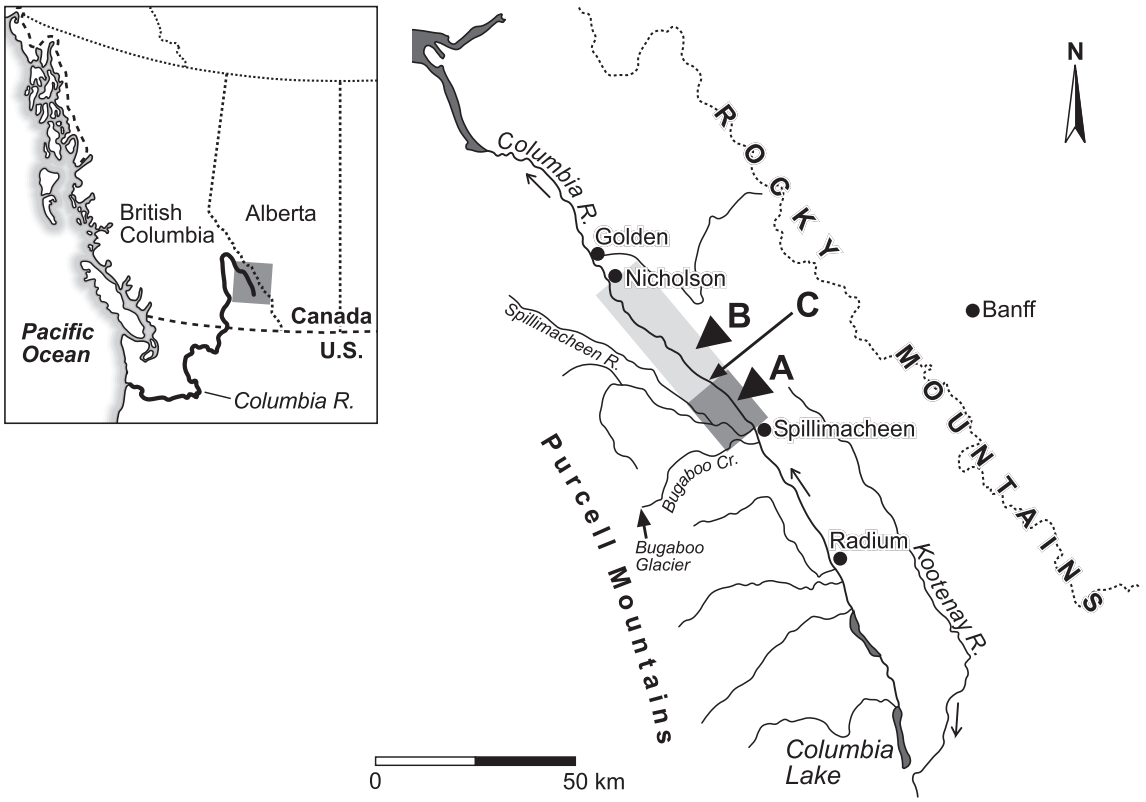

Fig. 2. The location of the upper Columbia River in south-eastern British Columbia, Canada. The dark grey zone indicates the upper, strongly anastomosing, reach; the light grey zone indicates the lower, weakly anastomosing, reach. Locations of the Harrogate (A) and Parson (B) borehole cross-sections (Fig. 6), and the Castledale cross-section (C) studied by Makaske *et al.* (2002) (Fig. 5) are also shown.

40 km long (main channel distance) and bounded on the lower end by a large cross-valley alluvial fan at Nicholson. Few crevasses exist in this weakly anastomosing reach with an average channel slope of 6·8 cm km^{-1} (Abbado *et al.*, 2005).

Based on the morphological and slope differences between the upper and lower reaches, and downstream fining of river bed material over the two reaches, Abbado *et al.* (2005) suggested higher aggradation rates in the upper reach as a driving force of more frequent crevassing and avulsion. These higher aggradation rates would be caused by high sediment input by the Spillimacheen River overloading the upper Columbia. High in-channel alluviation rates in the upper reach would cause loss of channel flow capacity, levée overtopping and crevassing and, eventually, avulsion and secondary channel formation. Thus, sediment overloading could be an upstream control of anastomosis, alternative to downstream control by aggrading cross-valley alluvial fans as proposed by Smith (1983). Makaske *et al.* (2009) tested the idea of upstream control for the present-day anastomosing system, using sediment transport measurements and calculations that cover two recent flood seasons, and showed that much more bedload is trapped in the upper anastomosing reach than in the lower anastomosing reach (Fig. 4). Bedload storage in the channel leads to bed aggradation and loss of channel flow capacity (Makaske *et al.*, 2009). Numerical modelling of the channel network confirmed this and additionally predicted that the tendency to anastomose will disappear over time when upstream sediment supply equals the transport capacity (Kleinhans *et al.*, 2012). The latter suggests that sustained anastomosis requires a forcing mechanism for in-channel bed aggradation.

In-channel bed aggradation is strongly linked to floodplain aggradation. With loss of channel flow capacity, channels will spill overbank more frequently and for longer periods causing an increase in floodplain sedimentation rates. In the short-term, sedimentation rates across the

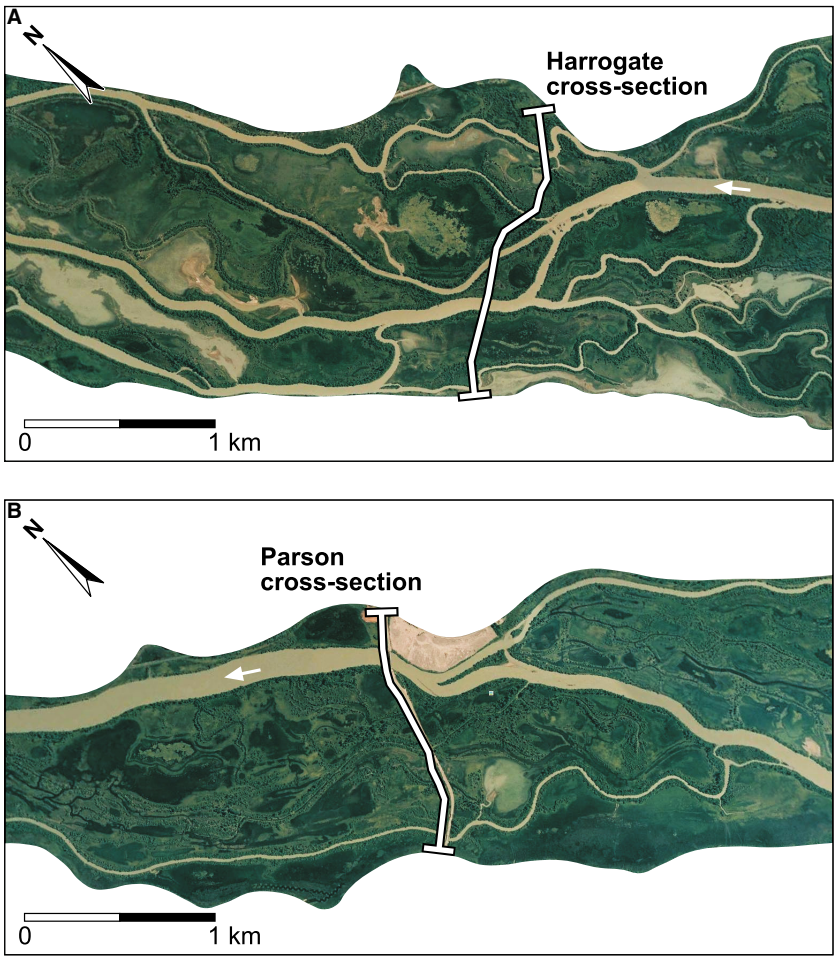

Fig. 3. The anastomosing river floodplain around the Harrogate (A) and Parson (B) cross-sections (panels A and B do not link up, but are *ca* 13 km apart). White areas along the floodplain represent mountain slopes and alluvial fans. Images from Google Earth (accessed in December 2010).

floodplain are strongly variable, with natural levée sedimentation rates exceeding floodbasin sedimentation rates some distance away from the channel belt (Törnqvist & Bridge, 2002). In the long-term, however, sedimentation associated with crevassing and avulsion will cause filling of the accommodation space created in the floodbasins (Farrell, 2001). Therefore, average long-term floodplain sedimentation rates for sedimentary sequences including deposits of multiple crevassing and avulsion cycles will not differ strongly across the floodplain.

An upstream or downstream forcing implies that floodplain sedimentation shows a downstream or upstream trend, which is investigated here relative to an earlier estimate. An average long-term floodplain sedimentation rate of 1·75 mm year^{-1} for the upper Columbia River was calculated for location C (Fig. 2) by Makaske *et al.* (2002). This rate was based on a radiocarbon date of seven *Scirpus lacustris* nuts buried by 7·9 m of upper Columbia floodplain deposits (Sample 3c in Fig. 5; Makaske *et al.*, 2002) and a time-depth analysis of many more, shallower, radiocarbon data (Makaske *et al.*, 2002, fig. 8) from a floodplain-wide borehole cross-section (Fig. 5). Besides dateable beds of peat and humic clay, this cross-section shows a number of channel sand bodies with associated natural levée and crevasse splay deposits (dominantly silty clay and sandy silt/clay in Fig. 5) in the subsurface testifying to at least nine avulsion events in the past 3000 years. Because the sampling site of Sample 3c of Makaske *et al.* (2002) is located in the middle of the valley and may be underlain by organic-rich beds of a substantial thickness, compaction may have influenced its vertical position. Therefore, the average long-term floodplain sedimentation rate for this location will be reconsidered in this paper.

METHODS

Fieldwork was carried out in the Columbia Valley in August and September 2009. Two floodplain-

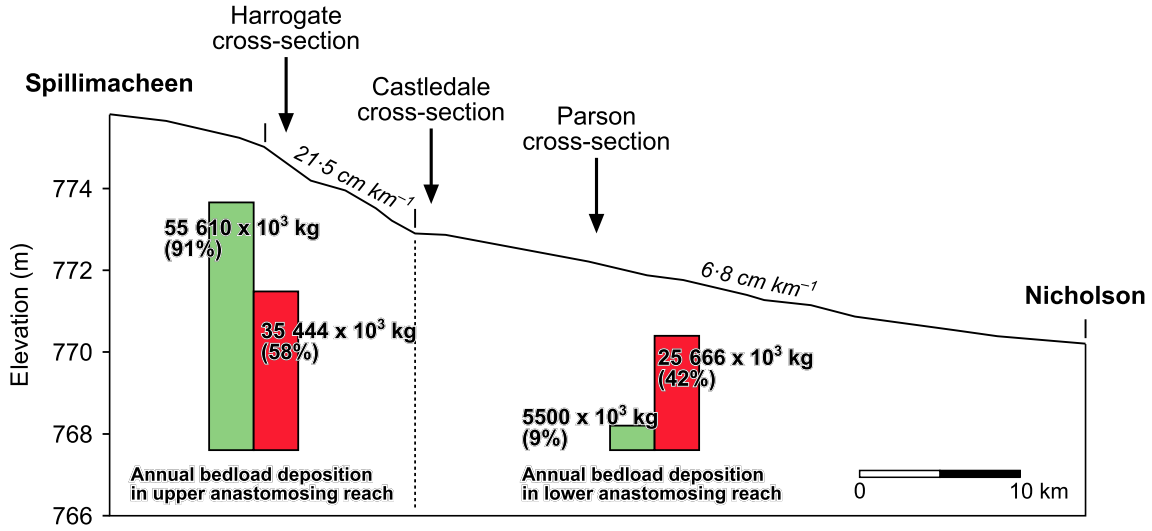

Fig. 4. Longitudinal profile of the upper Columbia River main channel between Spillimacheen and Nicholson (Fig. 2). Locations of the Harrogate, Castledale and Parson borehole cross-sections are indicated. Channel gradient data from Abbado *et al.* (2005) show a relatively steep upper reach and a relatively gentle lower reach. Vertical bars indicate estimates of the minimum and maximum amounts of bedload annually deposited in each reach, as calculated by Makaske *et al.* (2009) based on recent measurements. The green bars indicate a scenario in which 91% of the total amount of bedload deposited in the anastomosing reach is trapped in the upper reach, with the remaining 9% being deposited in the lower reach. The red bars indicate a more balanced scenario in which these values are 58% and 42%, respectively.

wide transects were investigated. One transect was located near Harrogate (Fig. 2), in the upper anastomosing reach; a second transect was located in the lower anastomosing reach near Parson (Fig. 2), *ca* 17 km downstream (valley distance). The transect previously studied by Makaske *et al.* (2002) is located near Castledale about halfway between both transects of this study, near the transition between the upper and lower anastomosing reaches (Fig. 4). In order to find suitable, deeply buried, floodplain organic material for radiocarbon dating to enable calculation of long-term sedimentation rates, 52 borings and two vibracorings were carried out. Borings were carried out using an Edelman auger and a gouge (Oele *et al.*, 1983). Because this equipment performs poorly in water-saturated sandy sediments, two vibracores were collected from the sandy fill of Channel 3 in the Harrogate transect using the equipment described by Smith (1984). The borings were spaced such that all natural levées, crevasse splays and floodbasins in the transects were sampled. Maximum boring depth was 8·7 m below the surface and sediment properties from the cores were described every 10 cm. Borehole locations were levelled relative to a local datum. The Harrogate cross-section was visited by boat, and the depth of navigable channels in this cross-section was determined by echo-sounding. The Parson cross-section was accessed by car, and the channel depth of channels 1 to 3 in this cross-section was measured with a rod. The depth of the main channel in this cross-section (Channel 4) could not be measured in this way. Lithological cross-sections (Fig. 6) were obtained by plotting and stratigraphic correlation of borehole logs. The minimum thickness of the beds depicted in Fig. 6 is 20 cm, for the sake of clarity.

Seven peat samples were collected for selection of material for radiocarbon dating. Sampling depth ranged from 4·2 to 6·7 m below the surface; sampling sites are indicated in Fig. 6. Seven sets of carefully selected terrestrial botanical macrofossils (such as *Carex* nuts) were submitted for AMS ^{14}C dating at the Centre for Isotope Research (Groningen, The Netherlands). Makaske *et al.* (2002) dated various fractions of organic-rich samples recovered from their boreholes and concluded that selected terrestrial macrofossils yielded the most reliable results. Therefore, in this study, only selected terrestrial macrofossils have been dated. The selection procedure described by Törnqvist *et al.* (1992) was followed, using a 150 μm mesh sieve. In this study, only botanical macrofossils were selected. Radiocarbon ages (Table 1) were calibrated using OxCal 4·2 (Table 2).

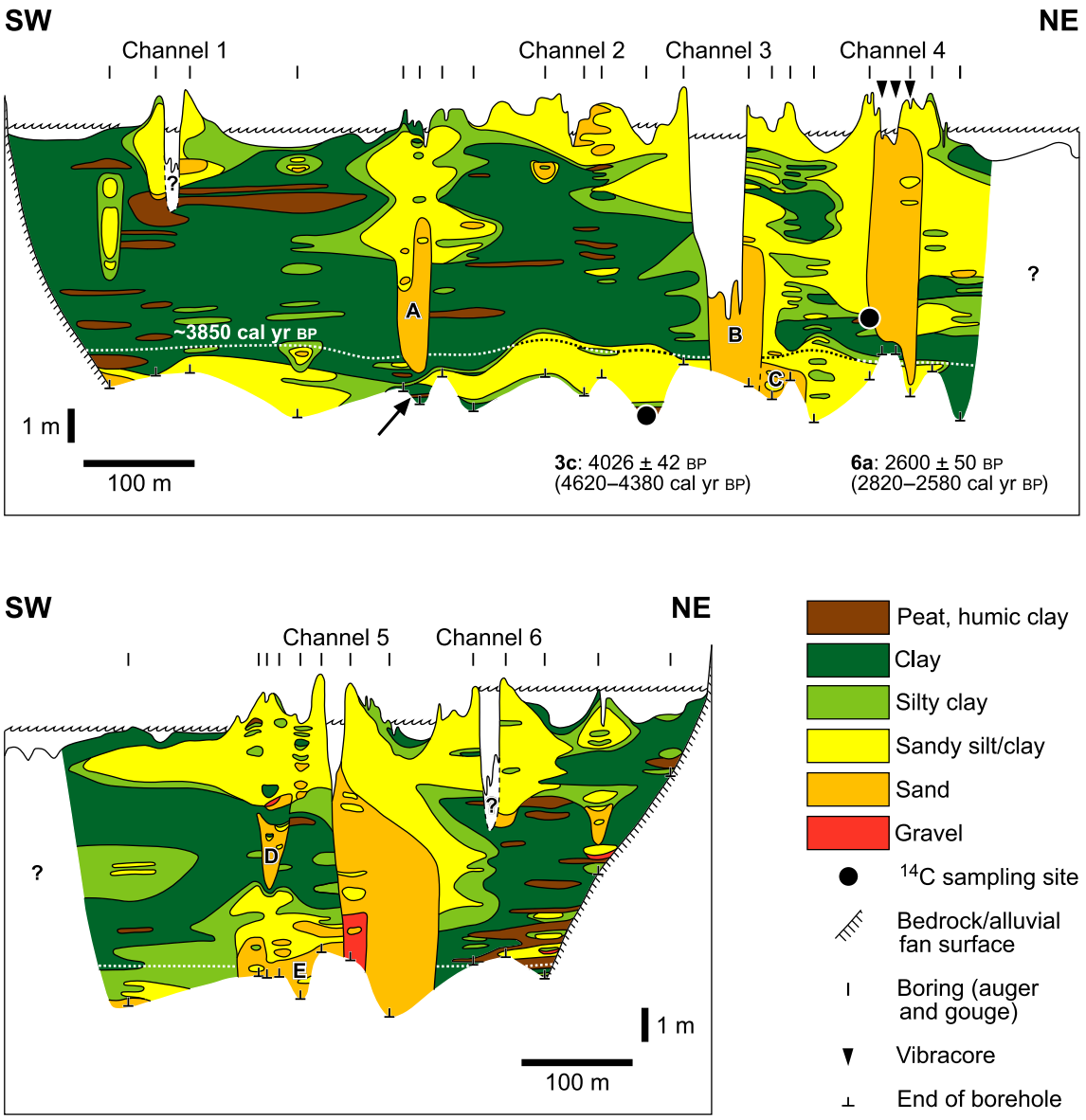

Fig. 5. The Castledale borehole cross-section of the upper Columbia River floodplain made by Makaske *et al.* (2002). Location of the cross-section is shown in Fig. 2. The stippled line in the subsurface represents the approximate position of the *ca* 3850 cal yr BP timeline. Positions of two ^{14}C-dated samples with ages (calibrated ages for the 2σ age interval) described by Makaske *et al.* (2002) are also shown. The black arrow in the upper panel (below sand body A) indicates a thin peat bed discussed in the text. The right-hand side of the upper panel links up to the left-hand side of the lower panel.

In order to minimize the influence of differences in compaction on long-term floodplain sedimentation rates, more or less compaction-free sampling sites were preferred. Along the valley sides, organic-rich beds rest on top of bedrock or coarse and/or consolidated alluvial fan deposits that can be considered as the compaction-free substratum. Sampling of these beds was preferred to sampling of organic beds underlain, or potentially underlain, by thick Holocene soft sediments and organic-rich beds (such as the site of Sample 3c in Fig. 5). This sampling strategy is analogous to the sampling strategy commonly followed in coastal areas for the reconstruction of Holocene relative sea-level rise, where basal peat on top of a steeply sloping sandy Pleistocene surface is sampled (e.g. Cohen, 2005; Berendsen *et al.*, 2007).

In addition to compaction, present floodplain topography may also influence calculated long-term average floodplain sedimentation rates, because sediment thickness to a radiocarbon-dated stratigraphic level tends to be greater

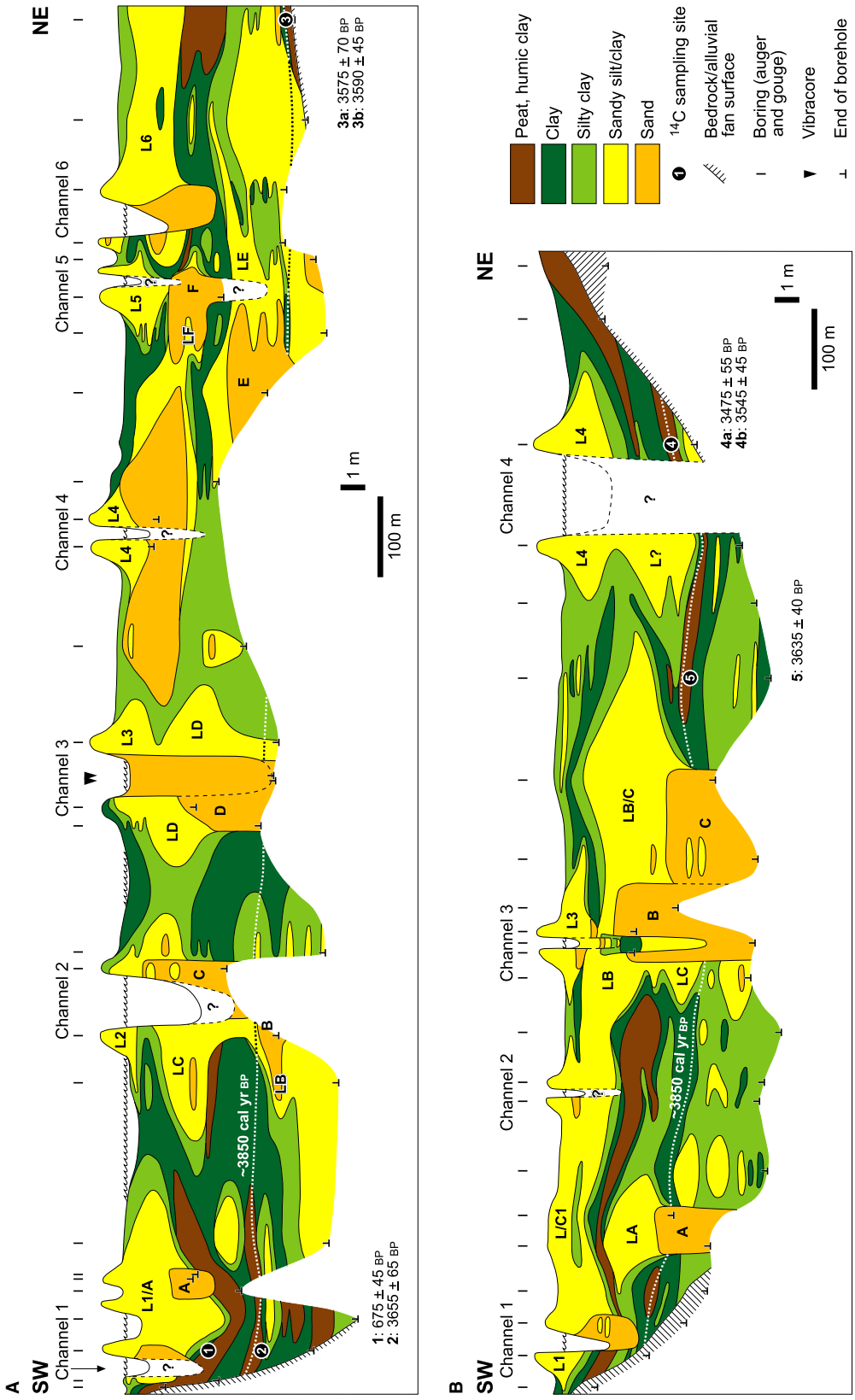

Fig. 6. Borehole cross-sections of the upper Columbia River floodplain made for this study showing subsurface lithology and stratigraphy and positions of ^{14}C-dated samples. Location of the cross-sections is shown in Fig. 2. The stippled line in the subsurface is the *ca* 3850 cal yr BP time-line. (A) The Harrogate cross-section of the upper study reach. (B) The Parson cross-section of the lower study reach.

Table 1. Radiocarbon age determinations from upper Columbia River floodplain material from the Harrogate and Parson cross-sections.

Sample	Laboratory no.	^{14}C age (^{14}C years BP)	Depth below surface (cm)	Material
Harrogate cross-section				
1	GrA-46792	675 ± 45	421–423	16 *Carex* sp. nuts
2	GrA-46797	3655 ± 65	644–646	23 *Betula* seeds, two *Myrica* seeds
3a	GrA-46795	3575 ± 70	670·5–673·0	One *Viola* sp. seed, one *Schoenoplectus lacustris* seed
3b	GrA-46793	3590 ± 45	668·5–670·5	Two Coniferae unspecified remains, four *Carex* sp. nuts, two *Schoenoplectus lacustris* seeds, two *Betula* seeds
Parson cross-section				
4a	GrA-46800	3475 ± 55	554–556	Six *Carex* sp. nuts, one Rosaceae seed, two *Galium* sp. seeds
4b	GrA-46566	3545 ± 45	552–554	Four *Salix* seeds/fruits, seven *Carex* sp. nuts
5	GrA-45815	3635 ± 40	522–524	25 *Schoenoplectus lacustris* seeds, 17 *Carex* sp. nuts

Table 2. Calibration of radiocarbon ages.

Sample	Laboratory no.	^{14}C age (^{14}C years BP)	1σ age (cal years BP)	2σ age (cal years BP)
Harrogate cross-section				
1	GrA-46792	675 ± 45	674–564	688–553
2	GrA-46797	3655 ± 65	4084–3895	4222–3784
3a	GrA-46795	3575 ± 70	3976–3731	4085–3654
3b	GrA-46793	3590 ± 45	3966–3840	4074–3726
Parson cross-section				
4a	GrA-46800	3475 ± 55	3831–3651	3886–3610
4b	GrA-46566	3545 ± 45	3898–3726	3966–3700
5	GrA-45815	3635 ± 40	4064–3891	4084–3846

beneath a natural levée than beneath a floodbasin. Therefore, in both cross-sections, sampling sites were located beneath natural levées and floodbasins.

FLOODPLAIN STRATIGRAPHY AND RADIOCARBON AGE DETERMINATIONS

The stratigraphy in the Harrogate and Parson cross-sections made for this study (Fig. 6) is broadly comparable to that of the Castledale cross-section (Fig. 5; Makaske *et al.*, 2002). Relatively narrow and thick channel-fill sand bodies occur in the subsurface of the upper Columbia floodplain and are associated with the present channels or are palaeochannel fills. Commonly, as a result of channel scour into palaeochannel fills in the subsurface, stacking of channel-fill sand bodies occurs (e.g. Makaske *et al.*, 2002, fig. 15). Wedge-shaped 'wings' of sandy clay and sandy silt are generally found on both sides of the present channels and are natural levée deposits. Often thick packages of sandy clay and sandy silt cover the top of palaeochannel-fill sand bodies, wedging out laterally on one or both sides of the sand body. These are final-stage channel and natural levée deposits, and may occasionally consist of sand and often grade laterally into silty clay. Channel-fill sand bodies and wedges of sandy clay and sandy silt are generally encased in a matrix of silty clay and clay, which are the floodbasin deposits. Occasionally, floodbasin deposits are split by laterally restricted peat and humic clay beds. Isolated, variously shaped, bodies of sand or sandy clay are interpreted as crevasse splay deposits. Below, the facies architecture of the

Harrogate and Parson cross-sections will be described and interpreted, building on the general picture sketched above. The ^{14}C sampling sites and age determinations will also be described for each cross-section.

Harrogate cross-section

In the Harrogate cross-section (Fig. 6A), Channel 1 is a small secondary channel that has bypassed the now abandoned Palaeochannel A. The sand bodies associated with Channel 1 and Palaeochannel A seem relatively small, although borehole information below Channel 1 is lacking. The sand bodies are encased in a *ca* 5 m thick and *ca* 250 m wide (width/thickness ratio of 50) lens-shaped body of sandy silt/clay (L1/A in Fig. 6A), of which the upper part dominantly consists of natural levée deposits, but of which the deeper parts probably consist of crevasse splay deposits related to the avulsive formation of Palaeochannel A. Palaeochannel A and its natural levées can still be recognized morphologically at the surface. Below lens L1/A, multiple organic beds occur in the subsurface. The upper organic bed seems strongly deformed by the overlying clastic lens.

Channel 2 is the main channel of the Harrogate cross-section. It has a width/depth ratio of about 18 (width *ca* 70 m, depth *ca* 4 m) and pronounced, but narrow, natural levées. Channel 2 has scoured into palaeochannel-fill C, which on its turn seems to have scoured into sand body B that is interpreted to be another palaeochannel fill. The stacking of channel-fill sand bodies is also recorded by a succession of lateral sandy silt/clay wedges that are separated by clay and organic beds. On the south-west side of Channel 2, the natural levée deposits of Palaeochannel C are represented by a *ca* 2 m thick sandy silt/clay wedge (LC) about 1 m below the recent natural levée deposits of Channel 2 (L2). A few metres lower, at the base of the section, the partly sandy upper part of a thick package of sandy silt/clay (LB) is interpreted to represent the natural levée deposits of Palaeochannel B.

Channel 3 is almost abandoned and filled with sand (Fig. 7). Its width of *ca* 40 m suggests that it is a former main channel, which probably started filling after the avulsive formation of Channel 2. Channel 3 has scoured into palaeochannel-fill D, which has its own lateral wedges of sandy silt/clay (LD) below the recent natural levée deposits of Channel 3 (L3). Vibracoring showed a 6 m thick sand fill below Channel 3, but it was not possible to distinguish the fill of Channel 3 from the fill of Palaeochannel D. A width/thickness ratio of ≤ 7 would apply if all vibracored sand is part of the fill of Channel 3.

Channel 4 is a small channel on top of a laterally extensive sand body that has a width/thickness ratio of about 140 (width *ca* 400 m, thickness 2·9 m). This sand body is interpreted as a large complex of crevasse splay deposits (Fig. 8 shows a presently active crevasse splay of comparable size). Channel 4 has probably

Fig. 7. Channel 3 in the Harrogate cross-section, which has almost completely filled with sand. Channel width is *ca* 40 m.

Fig. 8. A large sandy crevasse splay in the upper part of the upper Columbia River study reach, *ca* 5 km upstream of the Harrogate cross-section and *ca* 1 km downstream of the large Spillimacheen River tributary. In the proximal part of the splay, a crevasse channel has formed. In the distal part of the splay, a narrow sandy lobe crosses an abandoned channel (lined with trees) and has prograded into a floodbasin. Approximate view width in the middle of the photograph is 0·9 km.

developed from one of the crevasse channels on this splay. Due to a lack of deep borehole information below and near Channel 4, the depth of channel scour could not be determined. It is conjectured that Channel 4 is a relatively young channel that has not scoured through the underlying sand sheet. The natural levée deposits of Channel 4 on top of the sand sheet (L4) consist of sandy silt/clay and are 2 m thick on average.

Channel 5 is an abandoned channel that was partially reoccupied by a recent crevasse from Channel 6. Its modest size indicates that it was a secondary channel. A borehole on its pronounced south-western natural levée shows a 2·7 m thick wedge of mainly sandy silt/clay (L5), but gives no information about its potential channel-fill sand body. An older sand body (F) with separate, partly sandy, lateral wedges (LF) exists below Channel 5. Its base could not be reached, but based on its considerable minimum thickness it is interpreted as a palaeochannel fill. Another sand body (E) of unknown extent occurs in the deeper subsurface south-west of sand body F. A lateral wedge of sandy silt/clay (LE) extends from sand body F to the north-east. The geometry of sand body E could not be determined, but the limited borehole information already suggests a fairly substantial size and an associated palaeochannel.

The Harrogate section crosses Channel 6 directly downstream of the apex of a sharp bend, which is the downstream one of a couple of sharp bends (Fig. 3A). The channel is *ca* 35 m wide (the channel appears wider in Fig. 6 because of oblique crossing) and *ca* 3 m deep, giving a width/depth ratio of 12. The asymmetrical cross-sectional geometry of Channel 6, with the deepest part in the outer bend (i.e. south-west), is probably related to bend processes. Lateral as well as vertical migration of Channel 6 to the south-west is suggested by sandy channel deposits below the north-eastern (inner bend) natural levée. A *ca* 2 m thick package of sandy silt/clay (L6) extends from the natural levée of Channel 6 to the north-east. Two organic beds wedging out to the south-west were found below this package in the most north-eastern part of the cross-section. A 1·7 m thick bed of humic clay occurs at medium depth. At the base of the cross-section, a 0·2 m thick peat bed rests on the alluvial fan surface that rises to the north-east. The two organic beds are separated by a *ca* 3 m thick, laterally extensive, package of sandy silt/clay and silty clay that could represent either a crevasse splay or a natural levée of an unknown palaeochannel. Due to very poor accessibility, a narrow zone (about 100 m wide) on the edge of the floodplain was not included in the cross-section. Surface geomorphology in this zone and subsurface lithology in the most north-eastern part of the cross-section do not indicate palaeochannels running along the floodplain margin outside the cross-section.

In the Harrogate cross-section, dateable peat and humic clay beds occur along the valley sides (Fig. 6A), whereas large channels and

palaeochannel fills and related overbank deposits cluster in the central part of the cross-section. One sample for ^{14}C dating was taken from sampling site 1 (Fig. 6A), in the top of a relatively thick organic bed directly below a 4 m thick complex of mainly sandy clay and sandy silt. This sample yielded a relatively young ^{14}C age of 675 ± 45 years BP (Table 1). Three other samples in the Harrogate cross-section were collected from two deeper sampling sites between 6·44 m and 6·73 m below the surface on both sides of the floodplain (sampling sites 2 and 3, Fig. 6A). These samples yielded ^{14}C ages near 3600 years BP (Table 1). The two samples from sampling site 3 were taken from a thin peat bed directly overlying the alluvial fan surface. The sample from sampling site 2 represents the base of a peat bed covering a 2 m thick package of consolidated, laminated clay and silty clay, which onlaps the south-western valley side.

Parson cross-section

In the Parson cross-section (Fig. 6B), Channel 1 is a secondary channel with an asymmetrical cross-sectional geometry, related to bend processes. The section crosses Channel 1 downstream of the apex of a bend (Fig. 3B). A sand body was found below the north-eastern (inner bend) natural levée of Channel 1, which is interpreted as channel deposits of Channel 1 that have migrated laterally to the south-west (comparable to Channel 6 in the Harrogate cross-section). The outer bend natural levée deposits of Channel 1 consist of a 2·3 m thick wedge of silty clay and sandy silt/clay (L1 in Fig. 6B) resting on an organic bed that seems to have been cut by scour of Channel 1. North-east of Channel 1 a *ca* 2 m thick package of sandy silt/clay (L/C1) overlying the organic bed is probably natural levée and crevasse splay deposits. Underlying the organic bed is a palaeochannel sand body (A) capped by a 2·3 m thick package of sandy silt/clay (LA) wedging out and grading into silty clay laterally on both sides of the sand body. This package is interpreted as final-stage channel and natural levée deposits of Palaeochannel A. On both sides of sand body A, the lateral wedges (LA) are underlain by a clay bed, including a lens of organics to the south-west.

Channel 2 in the Parson cross-section is a small abandoned channel, which, judging from the floodplain geomorphology, seems to have been a crevasse channel branching from Channel 1 upstream of the cross-section. Channel 2 has scoured into the *ca* 2 m thick laterally extensive package of sandy silt/clay and silty clay (L/C1) that merges to the south-west with the natural levée deposits of Channel 1. This package is interpreted as a large complex of crevasse splay deposits existing between channels 1 and 3. Maximum scour depth of Channel 2 could not be determined, but its small size suggests very limited scour and only thin sandy channel deposits below the present channel base. The crevasse splay complex is underlain by a relatively thick (up to 1·6 m) organic bed that overlies the lateral silty clay wedge of Palaeochannel A (LA). At the base of the cross-section below Channel 2, an extensive metres-thick package of silty clay and sandy clay/silt exists that may be floodbasin, crevasse splay and natural levée deposits of an unidentified palaeochannel.

Channel 3 is a secondary channel that is presently abandoned. It has well-developed lateral wedges of sandy silt/clay (L3), partly underlying prominent, but narrow, natural levées. A borehole in the middle of the channel revealed a fine-grained channel-fill succession and no sand body associated with Channel 3. A large sand body (B), however, was found in the deeper subsurface and is interpreted as palaeochannel fill. It is covered by a sandy silt/clay bed that is separated from the lateral wedges of Channel 3 by a discontinuous clay bed. A clay plug in the top of sand body B can be interpreted as residual channel deposits, and it seems that Channel 3 has scoured into this clay plug, indicating channel reoccupation. Palaeochannel B has partly scoured into sand body C that represents an older palaeochannel. Sand body C seems relatively wide, but its actual width may be less because the section may obliquely cross the sand body that has no morphological expression at the surface. A metres-thick package of sandy silt/clay (LB/C) covers sand body C and wedges out laterally to the north-east. These are the final-stage channel deposits and natural levée deposits of Palaeochannel C that seem to have merged with the natural levée deposits of Palaeochannel B. South-west of sand body B multiple wedges of sandy silt/clay occur, with the ones at medium depth (LC) interpreted as belonging to sand body C.

Channel 4 is the main channel in the Parson cross-section. Its depth was not measured in the field, but estimated at 3 m based on a hydraulic geometry relationship established for the upper Columbia River by Tabata & Hickin (2003). With a width of *ca* 90 m, its width/depth ratio would be about 30. Channel 4 has 1·0 to 1·5 m high natural

levées with associated lateral wedges of sandy silt/clay (L4) in the subsurface. No channel-fill sand body was found near Channel 4, but this may be due to lack of borehole information below Channel 4. A lateral wedge of sandy silt/clay (L?; Fig. 6B) at medium depth below the south-west bank of Channel 4 may be natural levée deposits of a palaeochannel that was a predecessor of Channel 4. An organic bed runs beneath this wedge on both sides of Channel 4. Another organic bed occurs directly below the recent natural levée deposits of Channel 4 and drapes the alluvial fan surface constituting the valley side.

In the Parson cross-section, three samples were extracted from two sampling sites at 5·22 to 5·56 m below the surface (Fig. 6B). Sampling site 4 is situated in a thin peat bed near the underlying north-eastern valley slope, which consists of heterogeneous coarse alluvial fan deposits covered by a 0·6 m thick succession of sandy clay/silt, silty clay and humic clay. Sampling site 5 represents the base of a humic clay bed overlying a metres-thick package of clay and silty clay, at an unknown distance above the base of the valley fill. The ^{14}C ages of the three samples from the Parson cross-section are near 3550 years BP (Table 1).

SEDIMENTATION RATES

Floodplain sedimentation rates were calculated for the sediments overlying all ^{14}C-dated samples based on sample depth below the surface and calibrated age ranges (Table 3). Minimum and maximum rates were calculated based on different combinations of the extremes of the depth and age ranges.

Sedimentation rates calculated for the relatively young sample from sampling site 1 in the Harrogate cross-section are much higher than rates calculated for the other samples. This difference is attributed to lowering of sampling site 1 due to compaction of the underlying peat bed, upon rapid deposition of the clastic sediment wedge, associated with the avulsive formation of Channel 1 and/or Palaeochannel A (e.g. Van Asselen *et al.*, 2010). Sampling sites 2 and 3, however, are located near the compaction-free substratum, being either coarse and consolidated alluvial fan deposits or the bedrock valley side. It can be expected that compaction effects on the vertical position of samples from these sites are minimal. Therefore, these samples are considered suitable for calculation of long-term average floodplain sedimentation rates that are not distorted by local compaction effects. Long-term average sedimentation rates in the Harrogate cross-section amount to 1·50 to 1·81 mm year^{-1} (Table 3), with sampling site 3 yielding slightly higher rates than sampling site 2.

In the Parson cross-section, long-term average sedimentation rates of 1·26 to 1·52 mm year^{-1} were calculated for the sediment intervals above sampling sites 4 and 5. Because sampling site 5 is not located on the valley side near the compaction-free substratum, compaction of potential unknown organic-rich beds and soft sediments below the cross-section may have increased accommodation space above sampling site 5 relative to sampling site 4, and may have increased sedimentation rates relative to a situation without compaction. Nevertheless, long-term average sedimentation rates for sampling site 5 are slightly lower than for sampling site 4, which

Table 3. Long-term sedimentation rates in the Harrogate and Parson cross-sections.

Sample	Depth below surface (cm)	2σ age* (cal years BP)	Minimum sed. rate† (mm cal year^{-1})	Maximum sed. rate‡ (mm cal year^{-1})
Harrogate cross-section				
1	421–423	747–612	5·64	6·91
2	644–646	4281–3843	1·50	1·68
3a	670·5–673·0	4144–3713	1·62	1·81
3b	668·5–670·5	4133–3785	1·62	1·77
Parson cross-section				
4a	554–556	3945–3669	1·40	1·52
4b	552–554	4025–3759	1·37	1·47
5	522–524	4143–3905	1·26	1·34

*In this case: BP = before 2009. †Based on minimum depth and maximum (2σ) age. ‡Based on maximum depth and minimum (2σ) age.

may be due to the thick natural levée of Channel 4 overlying sampling site 4.

EVALUATION OF THE HYPOTHESES

Longitudinal trend in sedimentation rate

The calculated sedimentation rates suggest that long-term average sedimentation rates over the past *ca* 4000 years in the Harrogate cross-section are higher than in the Parson cross-section (Table 3; Fig. 9), with the minimum calculated sedimentation rate for Harrogate being slightly lower than the maximum calculated sedimentation rate for Parson. This result implies a downstream decrease in long-term average floodplain sedimentation rates and a validation of the hypothesis of dominant upstream control.

The Castledale cross-section (Fig. 5) studied by Makaske *et al.* (2002) is located about halfway between the Harrogate and Parson cross-sections (Fig. 2). With the hypothesis of upstream control in mind, it may be expected that the long-term average sedimentation rate at Castledale will be intermediate between the rates determined for Harrogate and Parson. The long-term average sedimentation rate calculated for the Castledale cross-section is 1·75 mm year^{-1} (time interval 4550 years), which is relatively high compared to the rates calculated in this study. The high rate of Makaske *et al.* (2002) heavily relies on a deep ^{14}C-dated sample, which was collected from the top a peat bed of unknown thickness in the middle of the valley (Sample 3c in Fig. 5). Unlike most of the sampling sites in this study, the vertical position of Sample 3c probably has been lowered by compaction of underlying peat. The strong deformation of the peat bed directly below clastic wedge L1/A in Fig. 6A demonstrates that clastic overburden may result in considerable compaction of underlying softer strata. Assuming that the peat bed formed nearly horizontal, because peat swamps are essentially flat topographic features, 1·5 m of compaction lowering of sampling site 1 seems to have occurred. In Fig. 5, it can be seen that Sample 3c is overlain by a *ca* 1·5 m thick clastic wedge of sandy silt/clay that thins to the south-west. A thin peat bed occurs below the wedge where it pinches out to the south-west (arrow in Fig. 5). The top of this of these peat bed is 0·4 m higher than the top of the peat bed from which Sample 3c was taken. If both of these peat beds are connected and underlie the clastic wedge similar to the bed below wedge L1/A in Fig. 6A, then at least 0·4 m of compaction lowering of the sampling site of Sample 3c seems to have occurred. However, the thin peat bed below the margin of the clastic wedge will also have been lowered by compaction since its formation, for example because of the overburden of palaeochannel-fill A. Estimating this compaction lowering conservatively at 0·1 m, a realistic estimate of compaction lowering of the sampling site of Sample 3c could be 0·5 m. Correction for this compaction lowering would result in a sedimentation rate of 1·63 mm year^{-1}, which would be close to that in the Harrogate cross-section, but even this corrected value probably overrates the long-term average sedimentation rate at Castledale. Based on the Makaske *et al.* (2002) data set, Makaske *et al.* (2009, fig. 10) inferred an average natural levée sedimentation rate of 1·65 mm year^{-1} for the Castledale cross-section. This value excludes rapid crevasse splay deposition associated with

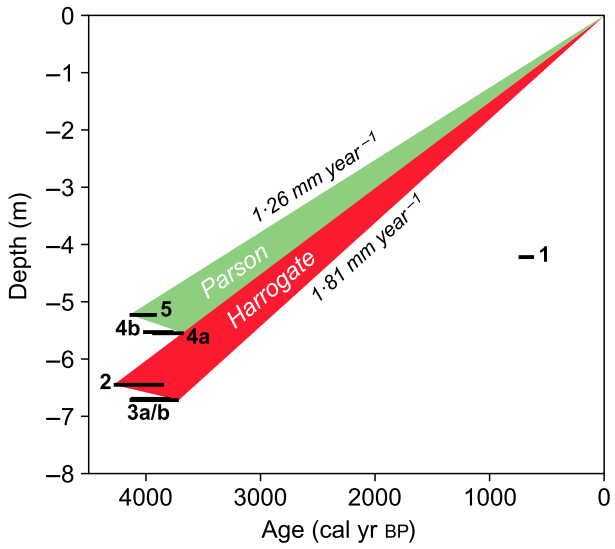

Fig. 9. Age–depth diagram with radiocarbon data from this study. Calibrated age of ^{14}C-dated samples is plotted against their depth below the surface at the borehole location. Width of the black bars represents the 2σ error range of the calibrated age. Age is given in calendar years BP, which in this case is before 2009 (the year of sampling). For the purpose of clarity, the thickness of the bars is slightly greater than needed to correctly represent the sample thickness. The red zone indicates the range of long-term sedimentation rates calculated for the Harrogate cross-section (Table 3). The green zone indicates the range of long-term sedimentation rates calculated for the Parson cross-section (Table 3). Note the divergent position of the bar representing Sample 1 associated with compaction (discussed in the text).

avulsive channel formation, which was taken as an explanation for the fact that the average natural levée sedimentation rate was slightly lower than the long-term average floodplain sedimentation rate of 1·75 mm year^{-1}. With the latter rate now being considered too high because of compaction effects, it seems much more likely that the real long-term average floodplain sedimentation rate in the Castledale cross-section is lower than the average natural levée sedimentation rate, because natural levées are relatively rapidly aggrading environments. Taking into account this additional information, a long-term average floodplain sedimentation rate, uninfluenced by compaction effects, of *ca* 1·5 mm year^{-1} for the Castledale cross-section, which would be intermediate between the rates for Harrogate and Parson, seems realistic.

Longitudinal trend in avulsion frequency

Part of the hypothesis of dominant upstream control of upper Columbia River anastomosis is the notion that high bedload input into the anastomosing reach could lead to bed aggradation, loss of channel flow capacity and an increased frequency of crevassing and avulsions. In this chain of events, high floodplain sedimentation rates are a final effect, resulting from an increase in avulsion frequency. If this notion is correct, the avulsion frequency in the Harrogate cross-section should be higher than in the Parson cross-section. Below, this part of the hypothesis will be evaluated.

Based on the ^{14}C dates for sampling sites 2 to 5, which are in the range of approximately 4000 to 3750 cal yr BP, and stratigraphic interpretation of the borehole data, the *ca* 3850 cal yr BP timeline has been drawn in the cross-sections herein, following the method of Gouw & Erkens (2007). In the Harrogate cross-section (Fig. 6A), the 3850 cal yr BP timeline runs directly above sampling site 2 (2σ range of ^{14}C date 4222 to 3784 cal yr BP). It then follows the organic bed to the north-east, where the stratigraphy suggests that it continues directly above sand body B, whereas it probably passes below the lateral clastic wedges of sand body D. In the north-east part of the cross-section, the ^{14}C dates for sampling site 3 (maximum 2σ range 4085 to 3654 cal yr BP) indicate that it will run more or less through this sampling site following the general stratigraphy to the south-west and therefore presumably passing beneath the lateral clastic wedge of sand body E. Its position beneath Channel 4 is unknown due to a lack of deep borehole information showing stratigraphy. In the Parson cross-section (Fig. 6B), the ^{14}C dates for sampling sites 4 and 5 (2σ range of all ^{14}C dates 4084 to 3610 cal yr BP) indicate that the 3850 cal yr BP timeline follows the peat bed underlying the lower clastic wedges below the natural levées of Channel 4, which also implies that the timeline runs below the lateral clastic wedges of Palaeochannel C. In absence of dating evidence, the stratigraphy to the south-west suggests that the 3850 cal yr BP timeline passes below the lateral clastic wedges of Palaeochannel A.

In order to determine the avulsion frequency in each cross-section, the number of channels formed since 3850 cal yr BP was determined by counting the number of channels and palaeochannel sand bodies having lateral wedges of overbank deposits above the timeline. In the Harrogate cross-section (Fig. 6A), the six present channels and palaeochannels A, C, D, E and F all have the base of their natural levée deposits above the timeline, which would imply that eleven avulsions have occurred in the past *ca* 3900 years. Eleven avulsions is considered a minimum value, because palaeochannel sand bodies may have been missed, due to low borehole density in the floodbasin between Palaeochannel A and Channel 2, and limited boring depth below the wide sand body below Channel 4. Also there is a slight chance that avulsions by reoccupation of abandoned channels have been overlooked, although a channel reoccupation usually leads to a clearly recognizable double pair of lateral clastic wedges. Avulsion frequency in the Harrogate cross-section can thus be estimated at ≥2·8 avulsions kyr^{-1} (Table 4). In the Parson cross-section (Fig. 6B), the four present channels and the three

Table 4. Avulsion frequency and average long-term floodplain sedimentation rate in three cross-sections of the upper Columbia River floodplain.

Cross-section	Avulsion frequency (avulsions kyr^{-1})	Sedimentation rate* (mm cal year^{-1})
Harrogate	≥2·8	1·50–1·81
Castledale	2·1 to ≥2·8	≤1·75†
Parson	1·3–2·1	1·26–1·52

*Average long-term floodplain sedimentation rate.
†The value of 1·75 mm cal year^{-1} (Makaske *et al.*, 2002) is probably influenced by peat compaction and therefore may be too high; see text for discussion.

palaeochannels A, B and C have lateral clastic wedges above the 3850 cal yr BP timeline, which would mean that seven avulsions have occurred in *ca* 3900 years. It may be argued, however, that Channel 2, which debouches in a floodbasin *ca* 0·5 km downstream of the cross-section, is a crevasse rather than an avulsion channel. Also the somewhat larger Channel 3 could be reinterpreted as a crevasse channel, because it debouches in a floodbasin 1 to 2 km downstream of the cross-section. On the other hand, a separate lateral wedge (L?; Fig. 6B) below the natural levée deposits of Channel 4 suggests a fourth palaeochannel that should be taken into account, with Channel 4 possibly having been formed by reoccupation of this earlier channel. Thus, the number of avulsions since 3850 cal yr BP is five at minimum and eight at maximum, which gives a frequency between 1·3 and 2·1 avulsions kyr^{-1} for the Parson cross-section (Table 4). These figures indicate that avulsion frequency in the past *ca* 3900 years has been significantly higher at Harrogate than at Parson, which fits with higher sedimentation rates at Harrogate and the hypothesis of upstream control of anastomosis by high bedload input.

In the Castledale section, the 3850 cal yr BP timeline runs between the sampling sites of Sample 3c (2σ range of ^{14}C date 4620 to 4380 cal yr BP) and Sample 6a (2σ range of ^{14}C date 2820 to 2580 cal yr BP) and thus above the sand body of Palaeochannel C. To the south-west, ^{14}C dates bracketing the timeline are lacking but stratigraphically the 3850 cal yr BP timeline can be expected to more or less overlie the sandy silt/clay and silty clay deposits in the deeper subsurface. To the north-east, stratigraphy suggests that the timeline cuts through palaeochannel sand body E and its lateral silty clay wedges. Channels 1 to 6 and palaeochannels A, B, D and possibly E have lateral wedges of overbank deposits above the timeline, indicating that ten avulsions may have occurred in this section since 3850 cal yr BP. The double pairs of clastic wedges associated with Palaeochannel A, however, suggest a reoccupation event of this channel, which would mean that the maximum number of avulsions since 3850 cal yr BP is eleven. This number may even be higher if channel sand bodies in the subsurface have been missed, for example below the large floodbasin between channels 4 and 5. The maximum avulsion frequency in the Castledale section therefore is $\geq$2·8 avulsions kyr^{-1}, which would be equal to the frequency in the Harrogate section. However, Channel 2 is a crevasse channel that may not develop into an avulsion, and the reoccupation of Palaeochannel A may also represent crevasse activity rather than avulsion. Additionally, the base of the clastic wedges of Palaeochannel E may be below the timeline, which would mean that the avulsion predates 3850 cal yr BP. A minimum number of avulsions in the past *ca* 3900 years can be estimated at eight, giving a frequency of 2·1 avulsions kyr^{-1}. In conclusion, the avulsion frequency for the Castledale section is unlikely to be higher than for the Harrogate section and almost certainly not lower than the avulsion frequency for the Parson section (Table 4), which is consistent with a downstream decrease in avulsion frequency and dominant upstream control of anastomosis.

FLUCTUATIONS IN SEDIMENT SUPPLY

Remarkably, the ^{14}C ages collected here are all near 3550 years BP. Because the four sampling sites in organic beds in two cross-sections are *ca* 17 km apart, this suggests a period of widespread peat formation in the upper Columbia Valley just after 4000 cal yr BP. Peat growth in this environment can be expected to occur during periods of reduced suspended sediment input. The stratigraphy in the cross-sections thus suggests a period of increased sediment input to have followed the period of widespread peat growth. A shallower level with more extensive organic beds occurs at about medium depth in both cross-sections. This level was dated only in the Harrogate cross-section at 675 ± 45 BP (Fig. 6, sampling site 1). This date agrees fairly well with two dates from organic beds in the Castledale cross-section yielding 430 ± 80 BP and 500 ± 50 BP (samples 4c and 5c from Makaske *et al.*, 2002). These organic beds at medium depth generally underlie natural levée and crevasse splay deposits of the modern channels. A comparable architecture of a recent clastic bed covering widespread peat beds was documented for the Rhine-Meuse delta by Gouw & Erkens (2007) and was shown to result from increased sediment supply due to deforestation in the hinterland (Erkens, 2009; Middelkoop *et al.*, 2010). In summary, the radiocarbon-dated stratigraphy suggests fluctuating sediment supply to the Columbia Valley.

Such fluctuations would lead to overfeeding and underfeeding of the river, which would explain the upstream control. The present study

identifies a possible cause in the hinterland for the fluctuations. At present, the main sediment-feeding system to the study reach is the Spillimacheen River, which drains a montane and partially glaciated catchment in the Purcell Mountains. On the millennia timescale, climatic fluctuations affecting the glaciated Spillimacheen catchment seem the prime driving force of fluctuations in sediment supply. The Bugaboo Glacier drains to the upper Columbia Valley via Bugaboo Creek (Fig. 2), which debouches into the upper Columbia River a few kilometres upstream of the Spillimacheen River. For the Bugaboo Glacier in the Purcell Mountains, a history of Holocene advances and retreats is documented by Osborn (1986) and Osborn & Karlstrom (1988). Neighbouring glaciers to the north-west of the Bugaboo Glacier are located in the Spillimacheen catchment, and their Holocene history can be expected to be very similar to that of the Bugaboo Glacier. Three distinct periods of middle to late Holocene glacial expansion have been reported for the Bugaboo Glacier, the last one being known as the Little Ice Age (*ca* 1100 to 1950 AD). The ^{14}C dates of organic beds in the upper Columbia Valley carried out for this study and by Makaske *et al.* (2002), plotted along with the glacial chronology, largely fall in intervening periods, but often near the transition to glacial expansion (Fig. 10). This pattern suggests that periods of increased sediment supply to the upper Columbia Valley are linked to periods of glacial expansion. In general, near glaciers most sediment becomes available for transport in periods of moraine deposition (i.e. during maximum ice cover) and in periods of ice retreat directly following maximum ice cover, because of exposure of large areas of unstable glacial deposits to fluvial erosion (e.g. Leonard, 1986). Such (accelerated) reworking of glacial deposits following deglaciation has been described as paraglacial processes (see Ballantyne, 2002, for a review). Additionally, periods of glacial expansion are likely to be colder, with reduced vegetation cover resulting in more unstable scree slopes in high altitude catchments and therefore higher sediment supply to rivers.

It seems very likely that floodplain sedimentation rates in the upper Columbia Valley have fluctuated on the millennia timescale in response to Holocene glacial cycles. During periods of reduced ice cover and glacial activity, sediment supply to the Columbia Valley must have been relatively low, allowing peat beds to develop in wet floodbasins further away from the channels, near the edges of the floodplain. Because peat growth probably was slow (in the absence of rapid base-level rise) and sedimentation continued near the channels, cross-levée gradients gradually increased and favourable conditions for avulsion developed during these periods. With the channels having been prepared for avulsion, increased sediment supply during and following glacial advances will probably have induced crevassing and avulsion

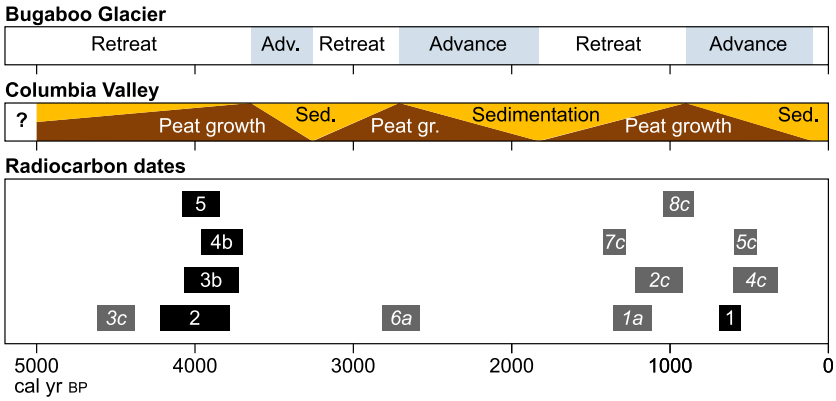

Fig. 10. The relationship between Neoglacial periods and Columbia Valley peat chronology. The upper panel shows periods of glacial advance (blue) and retreat (white) for the Bugaboo Glacier (Osborn, 1986; Osborn & Karlstrom, 1988). The middle panel shows inferred periods of glacially induced sedimentation in the Columbia Valley and intervening periods of increased peat growth. The lower panel shows ^{14}C dates of upper Columbia River floodplain organic beds, plotted as boxes indicating the 2σ age interval. When more dates from the same sampling site were available, the date with minimum standard deviation was chosen. Dark grey boxes indicate ^{14}C dates from Makaske *et al.* (2002, table 2); black boxes indicate ^{14}C dates from this study.

activity. A recent increase of avulsion activity can be recognized in the stratigraphy of the Harrogate cross-section (Fig. 6A) where lateral clastic wedges associated with a substantial number of present and recently abandoned channels (for example, channels 1 and 4 and Palaeochannel A) dominate the shallow stratigraphy, whereas at medium depth more extensive peat, humic clay and clay beds occur. The same holds for the Castledale cross-section (Fig. 5), although laterally extensive sand bodies, such as the one below Channel 4 in Fig. 6A, are absent here. In the Parson cross-section (Fig. 6B), the same phenomenon can be recognized, but with a reduced number of active channels. Radiocarbon-dated channel ages from the Castledale cross-section (Makaske *et al.*, 2002, fig. 9) indicate that channels 1, 2, 3 and 6 and Palaeochannel D all have been formed in the past millennium, i.e. the Little Ice Age, whereas stratigraphy suggests that Palaeochannel A has been reoccupied and a crevasse channel has been formed north-east of Channel 6 in the same period. Comparable dating evidence is not available for the Harrogate cross-section, but the ^{14}C date from sampling site 1 suggests that the majority of the relatively coarse-grained sediment bodies, and the associated channels and palaeochannels in the upper part of the section can also be linked to the Little Ice Age.

It may be that human activities in the catchment, such as deforestation and development of infrastructure, have also increased sediment supply in the 19th and 20th Centuries and therefore may in part be responsible for an increase in crevassing and avulsion activity. Because expansion of (European) human activities in the area largely coincided with the final stages of the Little Ice Age, in which sediment supply is believed to have greatly increased because of deglaciation, the potential human influence for this period cannot be separated from the glacial influence. The presently high sediment supply rates reported by Makaske *et al.* (2009) appear to be a logical phenomenon in the aftermath of both the Little Ice Age and a period of strong expansion of human activities. Consistent channel changes in the period since European settlement have been observed in other rivers in North America, but there too it has been difficult to unambiguously relate these changes to human impact (e.g. Joeckel & Henebry, 2008).

The recent sediment pulse associated with the Little Ice Age is likely to have affected the upper Columbia gradient line. The steep section in the upper anastomosing reach (Fig. 4) was interpreted by Kleinhans *et al.* (2012) as a result of sediment overfeeding in the past, which caused steepening to propagate into the anastomosing reach from the upstream boundary, i.e. the Spillimacheen–Columbia confluence. Their morphodynamic modelling could only reproduce the present-day longitudinal profile by temporary bed sediment overfeeding for a century. These authors concluded that increased avulsion frequency in the recent past may have been caused by a temporary disequilibrium between sediment feed and transport capacity. With the data presently available, it can be concluded that this period of temporary sediment overfeeding is very likely to coincide with the optimum and the final stages of the Little Ice Age. The steep section in the present-day longitudinal profile is approximately between the Harrogate and the Castledale cross-sections (Fig. 4), which means that the wedge of coarse sediment prograding into the reach from the Spillimacheen River is present in the Harrogate cross-section, but not in the Castledale cross-section. This recent sediment overfeeding could be reflected in the relatively coarse-grained and laterally quite extensive clastic wedges in the upper part of the Harrogate cross-section. It cannot be excluded, however, that the long profile also reflects sediment pulses from before the Little Ice Age, and that the present-day steep section thus has a composite nature.

IMPLICATIONS FOR DEPOSITIONAL SETTINGS AND FACIES MODELLING

The sedimentation rates and avulsion frequencies presented above support the hypothesis of dominant upstream control of upper Columbia anastomosis by long-term sediment overloading. Although this finding does not exclude the validity of downstream control by base-level rise for other anastomosing systems, it means a paradigm shift because the upper Columbia with its supposed downstream control has been influential as a modern example of anastomosis, frequently used to interpret ancient alluvial sequences. Upstream control of anastomosis fits with the foreland basin (e.g. Smith & Putnam, 1980; Kirschbaum & McCabe, 1992; Nadon, 1994; Plint & Wadsworth, 2003; Cuitiño *et al.*, 2015) and intramontane and intermontane basin settings (e.g. Bakker *et al.*, 1989; Dill *et al.*,

2003) of many interpreted subrecent/ancient anastomosing systems much better than downstream control. The present study indicates that the prime driving force of anastomosis in these settings is upstream control (sediment overloading) of the rivers entering the low-gradient foreland or intramontane basin, rather than downstream control associated with strong basin subsidence, as proposed earlier (Smith & Putnam, 1980; Smith, 1986; Makaske, 2001). Dominant upstream control implies that within such basins anastomosing systems tend to be best developed in the more proximal parts, instead of in the distal parts near the (local) base level. It also implies that anastomosing systems are akin to what have recently been called 'distributive fluvial systems' (Weissmann *et al.*, 2010).

However, with continued higher aggradation upstream, relative to downstream, anastomosing rivers will build up a higher gradient and, as a response, will acquire more energy to erode their banks and maintain channel flow capacity, in spite of high sediment loads. Consequently, the rivers will become less prone to avulsions and anastomosis will fade out.

Downstream control by base-level rise provides a mechanism to restore and maintain a low gradient in the basin under a high sediment deposition rate. Therefore, in the long-term, an anastomosing river can only continue to exist if

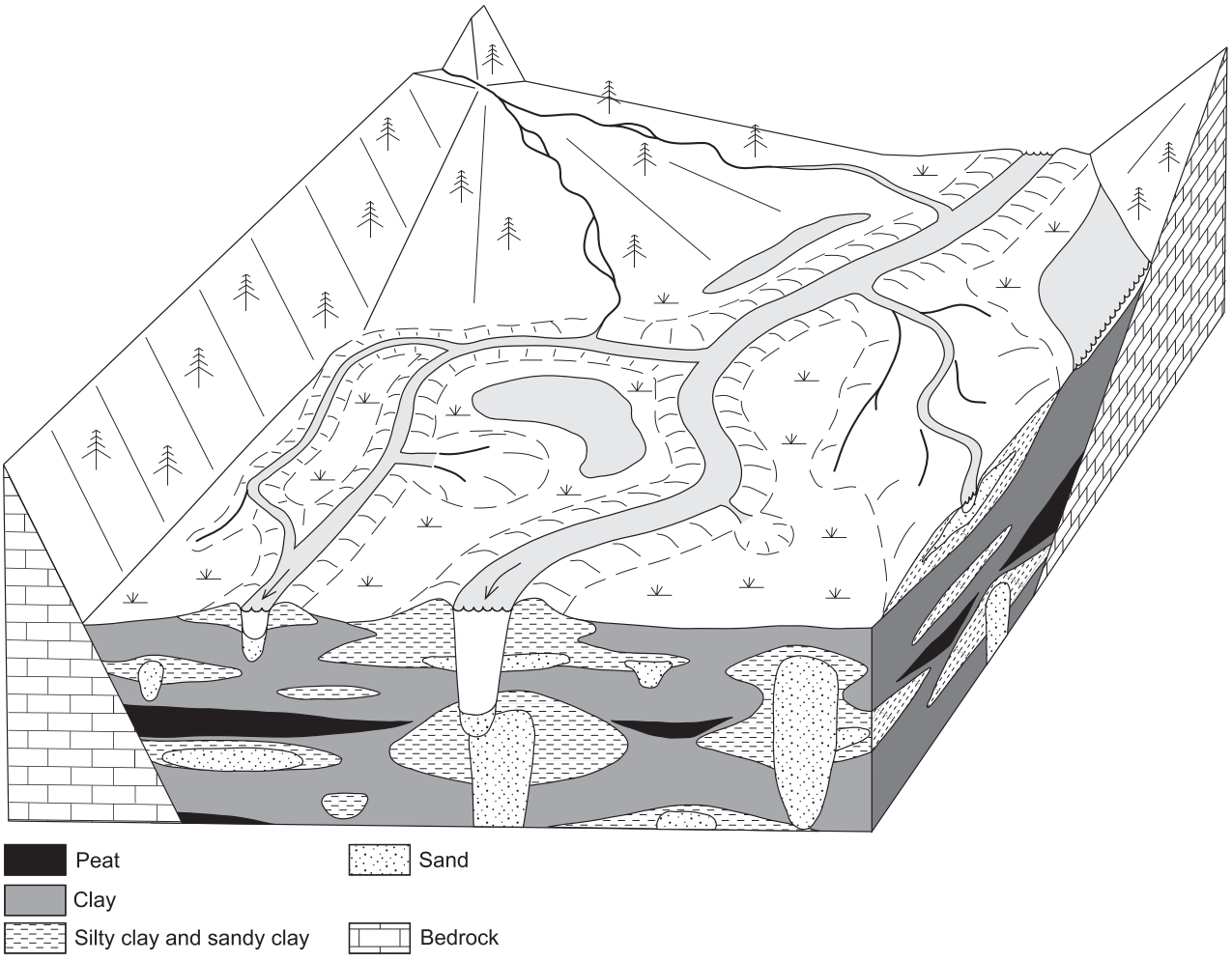

Fig. 11. Schematic block diagram of an anastomosing river in a temperate humid, intramontane (valley) setting (after Makaske, 1998, 2001) showing geomorphological elements and associated textural facies. The diagram shows the proximal part of the system directly downstream of a large alluvial fan, where anastomosis is well-developed. Because of high sediment loads entering the anastomosing river through the alluvial fan system, crevassing and avulsion is occurring in the proximal reach of the anastomosing system. Peat beds at medium depth of the exposed valley fill represent a period of reduced sediment supply and fluvial activity.

both upstream and downstream controls are involved. Thus, while high sediment supply is a primary cause of anastomosis, downstream control of relative base-level rise remains important as a secondary condition to maintain anastomosis over long periods of time. In the upper Columbia River, downstream control by base-level rise is probably attained as follows. Glacially driven enhanced sediment supply rates force anastomosis from upstream, but simultaneously increase the aggradation rates of the large cross-valley alluvial fan acting as a downstream boundary of the anastomosing reach. This mechanism helps to maintain a dynamic equilibrium between upstream sediment overloading as a primary control on anastomosis, and downstream base-level rise as a secondary control on anastomosis.

The results from this study on the controls of anastomosing systems, if valid for anastomosing rivers in general (which still needs to be investigated) have two important implications for facies modelling of anastomosing river basin fills. Firstly, with dominant upstream control anastomosing river deposits will show a distinct longitudinal facies-architectural trend. The proximal anastomosing river sequence will show a high proportion of channel and crevasse splay sand bodies and relatively thick and wide complexes of silty/sandy avulsion-related deposits encased in a clayey, possibly organic, matrix. The distal anastomosing river sequence will show a lower proportion of the coarse architectural elements, because of fewer avulsions and channels here. Secondly, with anastomosis being a disequilibrium form forced by fluctuations in sediment supply, thicker sequences of anastomosing river deposits will show an alternation of intervals dominated by fine, possibly organic, deposits and intervals with more abundant coarse-grained architectural elements. Depending on the forcing mechanisms, this alternation may be more or less regular. For example, Abels *et al.* (2013) demonstrated cyclicity of a fluvial intermontane basin fill caused by astronomically forced climate changes

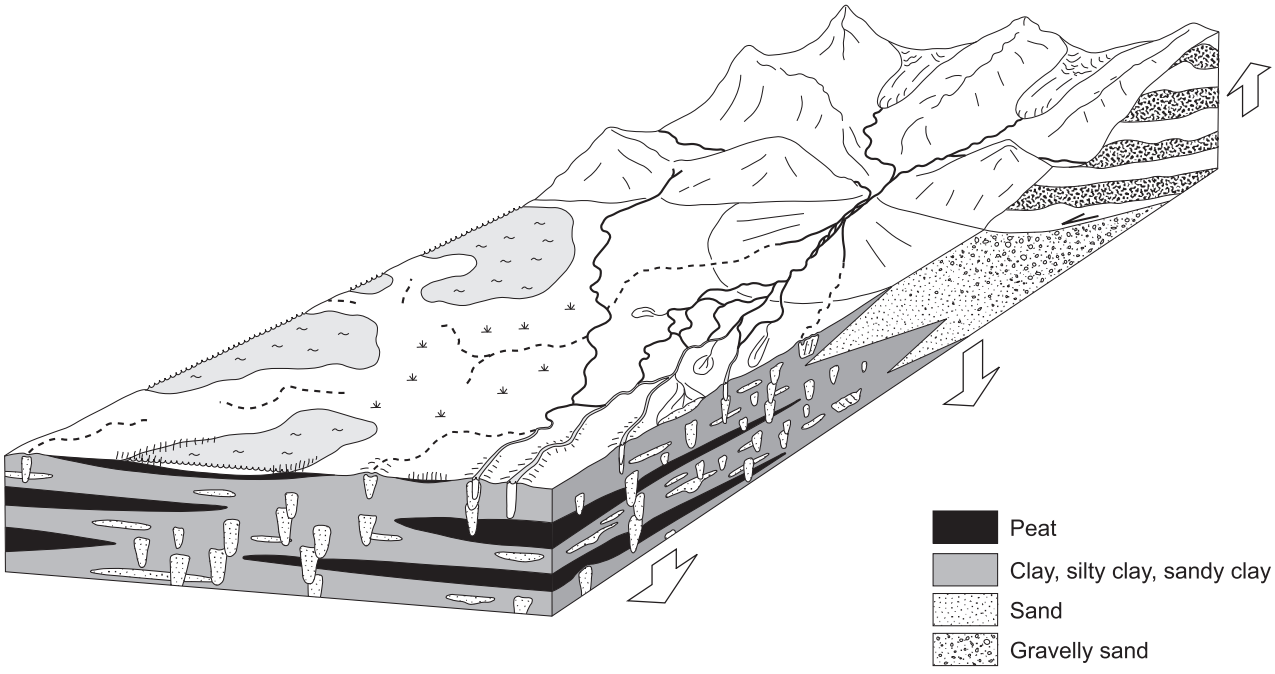

Fig. 12. Schematic block diagram of an anastomosing river system in a foreland basin showing geomorphological elements and associated textural facies. The diagram shows well-developed anastomosis in the proximal part of the basin, directly downstream of a fluvial fan, where sediment supply rates are relatively high. The system is fed from an uplifted and glaciated mountain catchment. An alternation of clastic and organic packages in the (distal) subsurface of the basin has formed in response to glacial fluctuations in sediment supply. Laterally extensive and predominantly clayey packages enclose variously shaped sand bodies being channel fills and crevasse splay deposits. Within the foreland basin, there is a downstream decrease in grain size, rate of basin subsidence and intensity of fluvial morphodynamics (including crevassing and avulsion activity within the anastomosing river system).

that led to recurrent large-scale reorganizations of the fluvial system. A less regular cyclicity in a montane setting may be caused by tectonics (e.g. Dill *et al.*, 2003).

In Fig. 11, the existing textural facies model for the upper Columbia River (Makaske, 1998, 2001) has been modified, taking into account the findings from this study. This figure only shows the proximal part of the anastomosing system, directly downstream of the alluvial fan system through which much sediment is supplied to the anastomosing reach. Downstream of the anastomosing reach a similar alluvial fan may provide a local base level. Based on the findings here in the intramontane upper Columbia River, a tentative textural facies model for anastomosing rivers in a large (foreland) basin can be worked out (Fig. 12), refining the early models for such settings as described by Smith & Putnam (1980) and Smith (1986). The model in Fig. 12 shows the longitudinal trend in sedimentary environments and related facies architectures in a glacially fed anastomosing system in a foreland basin. Both diagrams (Figs 11 and 12) apply to a temperate humid climatic setting, with glacially controlled sediment supply and potential for peat formation.

CONCLUSIONS

Anastomosing rivers are a major category of alluvial river systems of which the facies and sedimentary architecture are well-studied and understood. Much less clear and still a matter of debate are the controlling factors of the genesis of anastomosing rivers and the settings in which these controlling factors develop. Three conclusions following from this work contribute to a better understanding of controlling factors and settings and therefore have geological significance.

1 Upper Columbia River anastomosis is likely to be upstream controlled on the millennia timescale, as evidenced by downstream decreasing average floodplain sedimentation rates and avulsion frequencies over the past *ca* 3900 years. The underlying mechanism is that high bedload supply causes bed aggradation, loss of channel flow capacity and increased overbank flooding and floodplain sedimentation, as well as abundant crevassing and avulsions leading to formation of new channels. This mechanism of upstream control may apply to many other anastomosing rivers.

2 Sediment supply to the upper Columbia floodplain probably fluctuated in response to Holocene glacial advances and retreats in the hinterland, as indicated by extensive organic beds that formed during the final stages of glacial retreat. Increased supply of clastic sediments (and hardly any development of organic beds) is inferred for the final stages of glacial expansion and the early stages of glacial retreat. Raised avulsion activity, presumably because of increased sediment supply, occurred, for example, during the Little Ice Age (1100 to 1950 AD). Fluctuations in sediment supply and avulsion frequency strongly suggest that upper Columbia anastomosis is a disequilibrium feature caused by repeated disturbance of the fluvial system. In other systems, such fluctuations in sediment supply could be generated by non-glacial climatic fluctuations, tectonics and human interference.

3 Relatively proximal settings where abundant sediment is supplied to low-gradient floodplains appear to be favourable for development of anastomosing systems. These settings comprise intermontane and foreland basins. Thick sequences of anastomosing river deposits require prolonged low-gradient conditions, which can be achieved by base-level rise. Therefore, in addition to upstream control, downstream control remains an important secondary condition that can explain the occurrence of anastomosing systems over very long periods of time.

ACKNOWLEDGEMENTS

We appreciated the help of Hanneke Bos and Wim Hoek with selecting botanical terrestrial macrofossils. Financial support for this research was granted by the Netherlands Organisation for Scientific Research (NWO), Utrecht University and the Molengraaff Foundation. Funding by Alterra (Wageningen University and Research Centre), enabling presentation of this paper at the 10th International Conference on Fluvial Sedimentology (Leeds, July 2013), is gratefully acknowledged. The constructive reviews of Alessandro Ielpi and Vern Manville helped us to substantially improve this paper.

REFERENCES

Abbado, D., **Slingerland, R.** and **Smith, N.D** (2005) Origin of anastomosis in the upper Columbia River, British Columbia, Canada. In: *Fluvial Sedimentology VII* (Eds M.D. Blum, S.B. Marriot and S.M. Leclair), *Int. Assoc. Sedimentol. Spec. Publ.*, **35**, 3–15.

Abels, H.A., **Kraus, M.J.** and **Gingerich, P.D.** (2013) Precession-scale cyclicity in the fluvial lower Eocene Willwood Formation of the Bighorn Basin, Wyoming (USA). *Sedimentology*, **60**, 1467–1483.

Adams, P.N., **Slingerland, R.L.** and **Smith, N.D.** (2004) Variations in natural levee morphology in anastomosed channel flood plain complexes. *Geomorphology*, **61**, 127–142.

Bakker, J.G.M., **Kleinendorst, T.W.** and **Geirnaert, W.** (1989) Tectonic and sedimentary history of a late Cenozoic intramontane basin (The Pitalito Basin, Colombia). *Basin Res.*, **2**, 161–187.

Ballantyne, C.K. (2002) Paraglacial geomorphology. *Quatern. Sci. Rev.*, **21**, 1935–2017.

Berendsen, H.J.A., **Makaske, B.**, **Van de Plassche, O.**, **Van Ree, M.H.M.**, **Das, S.**, **Van Dongen, M.**, **Ploumen, S.** and **Schoenmakers, W.** (2007) New groundwater-level rise data from the Rhine-Meuse delta; implications for the reconstruction of Holocene relative mean sea-level rise and differential land-level movements. *Neth. J. Geosci./ Geol Mijnbouw*, **86**, 333–354.

Cohen, K.M. (2005) 3D geostatistical interpolation and geological interpretation of paleo-groundwater rise in the Holocene coastal prism in the Netherlands. In: *River Deltas; Concepts, Models, and Examples* (Eds L. Giosan and J.P. Bhattacharaya), *SEPM Spec. Publ.*, **83**, 341–364.

Cuitiño, J.I., **Ventra Santos, R.**, **Alonso Muruaga, P.J.** and **Scasso, R.A.** (2015) Sr-stratigraphy and sedimentary evolution of early Miocene marine foreland deposits in the northern Austral (Magallanes) Basin, Argentina. *Andean Geol.*, **42**, 364–385.

Davies, N.S. and **Gibling, M.R.** (2011) Evolution of fixed-channel alluvial plains in response to Carboniferous vegetation. *Nat. Geosci.*, **4**, 629–633.

Dill, H.G., **Khadka, D.R.**, **Khanal, R.**, **Dohrmann, R.**, **Melcher, F.** and **Busch, K.** (2003) Infilling of the Younger Kathmandu-Banepa intermontane lake basin during the Late Quaternary (Lesser Himalaya, Nepal): a sedimentological study. *J. Quatern. Sci.*, **18**, 41–60.

Erkens, G. (2009) Sediment dynamics in the Rhine catchment; quantification of fluvial response to climate change and human impact. *Neth. Geogr. Stud.*, **388**, 1–278.

Farrell, K.M. (2001) Geomorphology, facies architecture, and high-resolution, non-marine sequence stratigraphy in avulsion deposits, Cumberland Marshes, Saskatchewan. *Sed. Geol.*, **139**, 93–150.

Gouw, M.J.P. and **Erkens, G.** (2007) Architecture of the Holocene Rhine-Meuse delta (the Netherlands) - a result of changing external controls. *Neth. J. Geosci./Geol Mijnbouw*, **86**, 23–54.

Harwood, K. and **Brown, A.G.** (1993) Fluvial processes in a forested anastomosing river: flood partitioning and changing flow patterns. *Earth Surf. Proc. Land.*, **18**, 741–748.

Joeckel, R.M. and **Henebry, G.M.** (2008) Channel and island change in the lower Platte River, Eastern Nebraska, USA: 1855–2005. *Geomorphology*, **102**, 407–418.

Kirschbaum, M.A. and **McCabe, P.J.** (1992) Controls on the accumulation of coal and on the development of anastomosed fluvial systems in the Cretaceous Dakota Formation of southern Utah. *Sedimentology*, **39**, 581–598.

Kleinhans, M.G., **De Haas, T.**, **Lavooi, E.** and **Makaske, B.** (2012) Evaluating competing hypotheses for the origin and dynamics of river anastomosis. *Earth Surf. Proc. Land.*, **37**, 1337–1351.

Leonard, E.M. (1986) Varve studies at Hector Lake, Alberta, Canada, and the relationship between glacial activity and sedimentation. *Quatern. Res.*, **25**, 199–214.

Makaske, B. (1998) Anastomosing rivers; forms, processes and sediments. *Neth. Geogr. Stud.*, **249**, 1–298.

Makaske, B. (2001) Anastomosing rivers: a review of their classification, origin and sedimentary products. *Earth-Sci. Rev.*, **53**, 149–196.

Makaske, B., **Smith, D.G.** and **Berendsen, H.J.A.** (2002) Avulsions, channel evolution and floodplain sedimentation rates of the anastomosing upper Columbia River, British Columbia, Canada. *Sedimentology*, **49**, 1049–1071.

Makaske, B., **Smith, D.G.**, **Berendsen, H.J.A.**, **De Boer, A.G.**, **Van Nielen-Kiezebrink, M.F.** and **Locking, T.** (2009) Hydraulic and sedimentary processes causing anastomosing morphology of the upper Columbia River, British Columbia, Canada. *Geomorphology*, **111**, 194–205.

Middelkoop, H., **Erkens, G.** and **Van der Perk, M.** (2010) The Rhine delta: a record of sediment trapping over time scales from millennia to decades. *J. Soils Sed.*, **10**, 628–639.

Nadon, G.C. (1994) The genesis and recognition of anastomosed fluvial deposits: data from the St. Mary River Formation, southwestern Alberta, Canada. *J. Sed. Res.*, **B64**, 451–463.

Nanson, G.C. and **Knighton, A.D.** (1996) Anabranching rivers: their cause, character and classification. *Earth Surf. Proc. Land.*, **21**, 217–239.

Oele, E., **Apon, W.**, **Fischer, M.M.**, **Hoogendoorn, R.**, **Mesdag, C.S.**, **De Mulder, E.F.J.**, **Overzee, B.**, **Sesören, A.** and **Westerhoff, W.E.** (1983) Surveying The Netherlands: sampling techniques, maps and their application. *Geol. Mijnbouw*, **62**, 355–372.

Osborn, G. (1986) Lateral-moraine stratigraphy and Neoglacial history of Bugaboo Glacier, British Columbia. *Quatern. Res.*, **26**, 171–178.

Osborn, G. and **Karlstrom, E.T.** (1988) Holocene history of the Bugaboo glacier, British Columbia. *Geology*, **16**, 1015–1017.

Plint, A.G. and **Wadsworth, J.A.** (2003) Sedimentology and palaeogeomorphology of four large valley systems incising delta plains, western Canada Foreland Basin: implications for mid-Cretaceous sea-level changes. *Sedimentology*, **50**, 1147–1186.

Smith, D.G. (1973) Aggradation of the Alexandra-North Saskatchewan River, Banff Park, Alberta. In: *Fluvial Geomorphology: a Proceedings Volume of the 4th Annual Geomorphology Symposia Series held at Binghamton, New York, September 27–28, 1973* (Ed. M. Morisawa), pp. 201–219. State University of New York, Binghamton.

Smith, D.G. (1983) Anastomosed fluvial deposits: modern examples from Western Canada. In: *Modern and Ancient Fluvial Systems* (Eds J. Collinson and J. Lewin), Int. Assoc. Sedimentol. Spec. Publ., **6**, 155–168.

Smith, D.G. (1984) Vibracoring fluvial and deltaic sediments: tips on improving penetration and recovery. *J. Sed. Petrol.*, **54**, 660–663.

Smith, D.G. (1986) Anastomosing river deposits, sedimentation rates and basin subsidence, Magdalena River, northwestern Colombia, South America. *Sed. Geol.*, **46**, 177–196.

Smith, D.G. and **Putnam, P.E.** (1980) Anastomosed river deposits: modern and ancient examples in Alberta, Canada. *Can. J. Earth Sci.*, **17**, 1396–1406.

Tabata, K.K. and **Hickin, E.J.** (2003) Interchannel hydraulic geometry and hydraulic efficiency of the anastomosing

Columbia River, southeastern British Columbia, Canada. *Earth Surf. Proc. Land.*, **28**, 837–852.

Törnqvist, T.E. and **Bridge, J.S.** (2002) Spatial variation of overbank aggradation rate and its influence on avulsion frequency. *Sedimentology*, **49**, 891–905.

Törnqvist, T.E., **De Jong, A.F.M.**, **Oosterbaan, W.A.** and **Van der Borg, K.** (1992) Accurate dating of organic deposits by AMS ^{14}C measurement of macrofossils. *Radiocarbon*, **34**, 566–577.

Van Asselen, S., **Stouthamer, E.** and **Smith, N.D.** (2010) Factors controlling peat compaction in alluvial floodplains: a case study in the cold-temperate Cumberland Marshes, Canada. *J. Sed. Res.*, **80**, 155–166.

Weissmann, G.S., **Hartley, A.J.**, **Nichols, G.J.**, **Scuderi, L.A.**, **Olson, M.**, **Buehler, H.** and **Banteah, R.** (2010) Fluvial form in modern continental sedimentary basins: distributive fluvial systems. *Geology*, **38**, 39–42.

Manuscript received 3 March 2016; revision accepted 16 January 2017